Development of a Wearable Active Exoskeleton With Self-Aligning Mechanism

Ricardo Luís Nunes Andrade
ricardo.luis@tecnico.ulisboa.pt

Instituto Superior Técnico, Universidade de Lisboa, Lisboa, Portugal

***Abstract*—Diseases like cerebral palsy, stroke, or ataxia result in a vast array of symptoms and complications for the individual, such as asymmetrical/abnormal gait patterns, loss of balance, and muscle spasticity, which will require gait rehabilitation. Robotic devices like exoskeletons and orthosis aim to assist the user during gait rehabilitation, through both torque transmission and support. Despite the increase in research on these devices, the physical human-robot interface (pHRI) has not been properly developed, leading to high abandonment. An important factor behind this statistic is the onset of soft and musculoskeletal tissue injuries due to forces and torques at the interface. Within this work, the human-robot joint misalignment problem was addressed, which is, partly, the cause of spurious forces and torques at the pHRI. An experimental protocol was developed to assess misalignment, fixation displacement, pressure interactions, and user-perceived comfort in three different ankle foot orthoses, corresponding to three different pHRI designs. These were ankle-foot orthosis with a frontal shin guard (SOF), lateral shin guard (SOL), and the commercially available ankle modulus of the H2 exoskeleton. The SOF device showed reduced misalignment and related interactions and higher user-perceived comfort in comparison with H2 while improving the SOL device in pressure and comfort. Finally, five alignment solutions were designed and implemented in the SOF device. Within these, three were manual alignment solutions for vertical, horizontal and shin guard alignment, and two were kinematic redundancy solutions based on the release of the inversion/eversion of the ankle and the introduction of a prismatic joint.**

I. Introduction

Clinical physiotherapy remains the gold standard of rehabilitation after a disease that severely impairs the patient's musculoskeletal system [1]–[3]. Diseases like cerebral palsy, stroke, or ataxia result in a vast array of symptoms and complications for the individual, such as asymmetrical/abnormal gait patterns, loss of balance, and muscle spasticity. These subjects will require gait rehabilitation, where robotic devices of the lower limbs like exoskeletons and orthosis gained increased importance in the last decade [4], [5]. These devices act in parallel with the human body, not only guaranteeing a controlled environment for rehabilitation through the precision provided by robotics but a necessary relief for therapists by relieving them of repetitive, straining tasks, necessary for long-term recovery [4], [5]. Depending on the disease and the tasks at hand, these devices can be classified according to which joints and how many joints they support (via passive or active means) [6]. One of the main avenues by which robotic devices can be used in gait rehabilitation is by strengthening muscle action through torque transmission, thereby reproducing functional gait patterns and improving the symptoms through neuroplasticity. For instance, study [7] demonstrated that for both healthy and neurologically impaired participants there was an increase in metabolic cost (measured by VO2) from the baseline, indicating active therapy and muscle activation and, as such, clinical effectiveness of these devices for rehabilitation

Despite the increasing number of exoskeletons and AFOs being developed and the ones already available on the market, the interface between humans and robots has not yet been properly designed [8]. In fact, these devices have a high abandonment rate, with as much as a third of all devices being dropped by their user, with limitations in usability being the main hurdle for exoskeleton devices [9], [10]. Problems related to poor assistance given by the exoskeleton leading to the onset of fatigue, disturbance of normal movement patterns, and soft and musculoskeletal tissue injuries are recognized to be the main reasons for this statistic [10]–[13]. For anthropomorphic devices, defined in [13] as the devices "where any hinge corresponds to a degree of freedom (DOF) of the human limb", like ankle-foot orthoses (AFOs), a proper alignment of these hinges (or robotic joints) with the biological joints is paramount to reduce these effects [14]. In fact, it is widely agreed that this misalignment between the robotic and biological joints results in spurious forces and torques at the interface between human and robot, leading to discomfort, pain, or long-term injury [10], [11], [13]–[19]. It is, paramount that, in the development of these rehabilitation devices, the issue of misalignment is accounted for, measured, and corrected.

Within this paradigm, these issues should be addressed in the development of an AFO. The SmartOs project from the Biomedical Robotic Devices Laboratory at the University of Minho iterates on a device that currently exists in the market for research, the ankle module of the H2 exoskeleton [20], [21]. Within this project, research has found human-robot misalignment to be an important design flaw of this device [22], [23]. Two AFOs have been developed within this project that iterates on the H2 device and, through novel interface designs, intended to resolve the issue of misalignment [22]. It is, as such, important to assess which of the three different design philosophies for the physical human-robot interface (pHRI), the H2 and the two in-house devices, lead to less misalignment and interactions. This was done in section 3 of

this work. Finally, the knowledge from this assessment should be used to develop a new prototype that solves the underlying misalignment issues through dedicated alignment solutions, which is presented in section 4 of this work. Within the scope of the research done, no previous study has assessed all three of misalignment, interactions, and user-perceived comfort of an AFO in the same study, as well as used this assessment to compare different pHRI designs.

II. Related Work

A. Human-Robot Joint Misalignment

A crucial feature of the development and design of wearable assistive robotics is the human-robot interface (HRI). This is because, in most cases, the purpose of a wearable exoskeleton is to apply loads to the human musculoskeletal tissue, both through passive support and active torque transmission [6]. The transmission of these loads is mediated at the interface between the user's soft tissues and the device's mechanical supports. Within this interface, pressure and sheer loads are applied to the user. A narrative review on adverse effects in stationary gait robots (devices that support the user through a harness [24]) found that the top two most occurring adverse effects are either soft tissue or musculoskeletal related. Among these adverse effects, most are soft tissue related, like bruising, irritation and skin abrasion [11]. The same study pointed to cuffs and straps as responsible for some of these injuries. A similar study in overground exoskeletons (ambulatory devices that assist the user during walking over different surfaces and settings [25]) found, similarly, that most of the adverse effects were correlated with soft tissue injuries [26]. Both studies identified both soft and musculoskeletal tissue adverse effects as primary risk factors for exoskeleton use. Literature also differentiates soft tissue interactions.

The kinematic compatibility between the user and the robot is the most fundamental part of exoskeleton design to solve these interactions [6]. This represents the notion that the mechanical design of the exoskeleton (even before implementing actuation, and control strategies, among other technologies) should aim to ensure comfort, safety, and adequate wearability.

Anthropomorphic devices, such as the ones explored in this work, have to fully replicate biological DOF. For this purpose, an exact knowledge of human joint kinematics and the location of the instantaneous center of rotation (ICR) of the joint is necessary to properly transmit the required loads and torques [14] and to guarantee that neither system (the human or robot) restricts each other's movements [27]. This requirement, nevertheless, leads to four main causes of misalignment, as described by [13]: initial offset between both joints; migration of the biological ICR during gait; kinematic mismatch; and movement mismatch.

There is an intrinsic relation between misalignment, cuff rotation/displacement, and spurious pressure/sheer forces, as described in figure 1. Figure 1 shows three different cases that describe the relation between joint misalignment and fixation movement. In the first case, there is perfect alignment, with ideal torque transmission from the robotic device to the user, which is impossible to achieve. In figure 1 (b) rigid fixations are considered (no relative movement between the two) and an initial misalignment of magnitudes x and y. This misalignment leads to a resulting force F_res due to the acting torque T_act. Finally, figure 1 (c) presents a more realistic situation where due to the compliance of fixation (both the cuff material and soft tissue are compliant) relative movement between the two chains is allowed. Thus the same x and y misalignment cause a movement L of the cuff and a rotation γ relative to the skin.

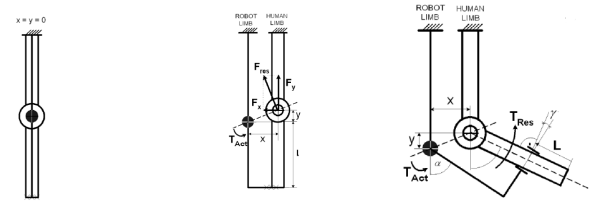

(a) Perfect alignment case. (b) Full rigid attachment case. (c) Realistic attachment case.

Fig. 1: Schematic of the misalignment and its effects. Taken from [16].

Finally, study [10] highlights the pressure and sheer force hazards resulting from an unappropriated human-robot joint alignment. This study further identifies misalignment as a safety hazard of rehabilitation robots. Literature shows significant efforts to assess misalignment and its effects, to guide the design process of an alignment solution. Research efforts in this field can be divided into three types: a) directly assess misalignment; b) directly assess interactions; c) indirectly assess interactions.

Direct misalignment assessment is not common in the literature. Within the scope of the research done, only two very recent studies quantified misalignment through motion capture [19], [28]. Study [28] quantified the misalignment of a knee brace by involving a dummy limb. In this study, motion capture was used to assess only rotation misalignment. On the other hand, [19] performed sit-to-stand tests on human subjects with an active knee exoskeleton. In this study, both x and y directions were captured, providing a 2D assessment of misalignment. This study provided interesting results for misalignment assessment (both initial and its variation during gait), showing that even in what was considered an ideal case there was still misalignment between the two joints.

Direct assessment of interactions is more commonly applied to assess misalignment effects. This can be done at the level of the soft tissue or the musculoskeletal tissue. At the level of soft tissue, both forces (pressure and shear) and moments can be measured. The main purpose of assessing pressure forces is to perform safety validation of a given HRI design [10], being relevant to measure the pressure values and their distribution. With this in mind, force-sensitive resistor (FSR) sensors are commonly used. These sensors are made of a material that changes its internal resistance when a force is applied. Study [29] installed a single FSR at 16 different HRI of a lower limb exoskeleton to assess regions of significant pressure

for three different movements and the main differences in pressure peaks for these movements. The study was successful in capturing these results in real-time. Furthermore, the same study successfully identified peak pressure differences between movements and interfaces. A similar study [30] used the same technology in conjunction with electromyography to determine the relationship between these interaction forces, muscle activation, and relative movement between the exoskeleton and the user. They found that the pressure measured by these sensors is largely due to exoskeleton movement. Finally, the study [31] used FSRs throughout the lower limb exoskeleton to verify if these pressures were lower than the pressure pain thresholds (PPT)s. PPTs are defined as the pressure threshold above which the pain caused is unbearable for the user [6]. This study shows that FSR use is valid to assess the real-time pressure and to compare peak values with those from the literature. Interactions at the interface can also be assessed in more than one axis DOF. Force-transducer-based technology is still the most robust and reliable way to capture the force exchange between the user and the device [10]. While these are not placed directly at the interface, 3 or 6-axis load cells can be fitted into the exoskeleton structure to capture three types (one normal and two sheer forces) or six types (one normal, two sheer forces, and three moments) of interactions [8], [17], [19].

Direct assessment of interactions at the musculoskeletal level is still a challenge due to the invasive nature of measuring the stress in bones and joints. The options tend to rely on instrumented dummies [28]. However, replicating the conditions of a normal human-device interface remains a challenge. As was described before, much of the misalignment problem is due to a kinematic mismatch between the robotic and biological joints, and the behavior of these biological joints is still not well understood. As such, the development of an instrumented dummy with simplified joints is not an option, since it would solve part of the mismatch that could lead to the interactions being measured. As such, a valid measurement system for musculoskeletal interactions has not yet been developed. A wrap-up of the state-of-the-art of direct interaction assessment at the HRI can be done from [32] which reviewed 33 studies on Human-Device interface measurement, comprising 9 exoskeletons, 7 orthoses, and 17 prostheses. Regarding the type of load measured, all studies measured pressure loads, while a fraction of these (around 15%) also measured sheer loads. No study measured only the latter, which strengthens the previous analysis made on the difficulty of assessing sheer forces interactions. Of the 33 studies, the FSR was the most used sensor (11 studies), forward by fiber optic, and the F-scan/F-socket sensors (a matrix-based sensor from Tekscan, Norwood, MA, United States), with 5 studies each. Of the 5 studies that addressed sheer interactions, 3 of them used strain gauges, 1 a capacitive sensor, and 1 a tri-axial force transducer, all custom-made for the given studies. The fact that 16 out of the 33 studies (the largest group of sensors) used FSR-based technology shows that, overall, they are a more robust and consolidated technology.

Moreover, sheer forces have a larger effect on soft skin injuries [10]. This fact consolidates the need for indirectly assessing these sheer forces. Displacement is measured through motion capture analysis in two different studies. [33], [34]. Even though the capturing technology is the same as for capturing misalignment, there is no need for model building or kinematic calculations. In fact, the main theory behind the following studies is that a fixation displacement, i.e., relative movement between a strap/cuff and the human soft tissue, will lead to these interaction forces. This displacement is measured by subtracting the positions of a marker in the user's limb and a marker in the fixation system (strap/cuff). A study [35] measured deformation on a lower limb walking orthosis. In this study, motion capture data was used to assess marker positions and, from these positions, angular variations between structural segments of the orthosis. As such, the method is capable to detect even small deformations in a rather rigid orthosis, with distances between markers as small as 3.2 mm being captured. Another study [33] used the same theoretical basis to capture displacements in an exoskeleton for the hand and wrist. The scale of the experiment was in millimeters, with displacements ranging from 0.2 to 40 mm, with a mean noise level of 0.23 mm and an upper limit (95% confidence interval) of 0.59 mm. This study gives a clear indication that this method can be used not only for small initial distances but also for small displacements. [34] used the same method but to assess the displacement of the cuffs of a physician assistant robot, which was then used to estimate interaction forces through a mathematical model. In this case, markers were used to capture the angle of each link of the robot, since the cuffs were connected to these links. Before each trial, the initial cuff position was captured in relation to each link. Afterward, the cuff position was traced by monitoring each link's position. This is an alternate method from [33] which, in theory, can be more robust. Since it is not based on the position of a single marker, it will suffer less from occasional errors like marker drift or dislodging. These studies show that fixation displacement can be properly assessed from motion capture data and that this method is valid for displacements of a magnitude of a couple of millimeters.

B. Alignment Solutions

A review of alignment studies [13] states three requirements these solutions should have. The first is kinematic compatibility, of which the same study [13] states that alignment solutions should introduce elements that allow for better initial and during gait alignment and should not restrain the biological ROM of the user. The second requirement is metabolic benefit. Implemented solutions should be designed to be lightweight and compact, such that they do not compromise the intended metabolic benefit the exoskeleton provides to the user. This can happen when the solution either significantly increases the robot's inertia (reducing transmission efficiency) or frees certain DOFs in the kinematic structure, where part of the torque will be transferred to.

The final requirement is that they should not compromise

the user's acceptance. One of the reasons for reduced user acceptance of assistive devices is a lack of consideration for the user's opinion and an incorrect assessment of the user's needs and priorities [9]. According to [13], important aspects related to user acceptance are effectiveness, durability, safety, and comfort, which should be taken into consideration when designing assistive devices.

Effectiveness is related to how well the device reaches its main goal (metabolic benefit) and how little it hinders the user (kinematic compatibility). Durability is that the device should be robust and durable and require low maintenance. Safety is directly related to the health risks the device might pose to the user. As such, alignment solutions should not compromise other aspects of the user's safety. The final aspect is comfort. Even if a device is perfectly safe, durable, and effective, users are more likely to not use a device that is uncomfortable or obtrusive.

A narrative review of available alignment solutions in the literature has divided these solutions according to their working principles into three types: Manual alignment; Use of Compliance Elements; and the addition of kinematic redundancy.

Manual alignment solutions are the simplest to design [13]. The strategy behind this implementation is that the robotic joint location can be changed according to the user's joint location. This can be done horizontally, vertically, or even by rotating the structure. This design mostly addresses macromisalignments, since it is not feasible for structures to allow for adaptation of a joint's location of more than half a centimeter at a time. Furthermore, the main challenge behind this design is correctly identifying the biological joint's location. This process will always carry a narrative error since it is not possible to determine the exact ICR of a joint due to the tissues that cover it [6], [13], [17]. Furthermore, the slippage of cuffs and braces that connect the user to the robot, coupled with the natural compliance of the skin, will further alter the joint's position and remove part of the alignment this solution initially provided [36], [37]. While a skilled operator, with knowledge of the relevant anatomical landmarks, can provide good results [38], studies have shown that, even with proper alignment, there is always some misalignment. Study [18] reported misalignments of 10 cm, while [19] reported vertical misalignments of around 5 cm and horizontal misalignments of around 3 cm. This solution does not cover the micromisalignments that come from a kinematic mismatch between the two joints or from the migration of the joint's ICR.

The introduction of compliant elements is another strategy. This can be done either at the structure/fixation level (frame and brace) or at the joint level. At the brace level, the idea is not to solve misalignment but rather to reduce its effects by changing the characteristics of the interface. A more compliant material at the interface has been shown to reduce the forces directly transferred to the user [17]. Compliance can also be incorporated at the level of the frame. The principle is to allow some deformation (effectively releasing a DOF with a small ROM) at the structure level. These solutions allow for reducing misalignment during gait (e.g. by allowing the device to follow the normal movement of the user's limb). Compliance can also be implemented at the joint level where the initial single DOF mechanism is replaced by a compliant coupling. This releases DOFs since the connection is now able to deform, which can be accomplished usually by using shape-changing materials. These DOFs have necessarily small ROMs [13].

The most complex strategy in alignment solutions is adding kinematic redundancy in the exoskeleton's kinematic chain [13]. This type of solution has been given increased attention [16], [18], [39], [40]. The working principle is that by adding more DOFs to the structure of the exoskeleton than the ones actuated it can better approximate the kinematics of the user. These mechanisms can allow for movement of the exoskeleton in relation to the user, in order to unload the user of the interactions of joint misalignment or decrease kinematic mismatch by releasing additional DOFs. Contrary to brace and frame compliance, these DOFs are usually implemented in series with the actuated DOF and have larger ROMs. These solutions can be implemented with two different rationales. One is when there is a need to match the kinematics of the human limb, so the fixations follow the user's movements. The intent is to solve the problem of hyperstaticity, where incorrect alignment leads to restrained mobility of the kinematic chains [14]. Another is when, either through analysis of the system kinematics or previous experiments, there is some knowledge of the movement at the fixations and, as such, the added DOFs compensate this movement.

A parallel avenue for addressing misalignment problems is through the development of soft or compliant exoskeletons, commonly denominated exosuits. Compared to the three kinematic structures before, which pertain to rigid exoskeletons, soft exoskeletons use soft and compliant structures at three levels: actuation, structure, and interface fixation [41], [42]. These exoskeletons are made up of an integrated garment that attaches to the body, a textile that is responsible for force transmission and actuated segments [41]. However, soft exoskeletons have not performed better than conventional rigid exoskeletons in a rehabilitation setting [41].

Finally, a narrative review of the literature was also done. This review found 25 reports describing 19 different devices, between exoskeletons and orthosis, that included an ankle joint with alignment mechanisms. An analysis was done regarding their actuation method, alignment solution, and distal mass. Of the 19 devices, 6 (approximately 32%) were based on soft structures. Of the remaining 13, all implemented manual vertical alignment, 69% implemented kinematic redundancy solutions, and 61% implemented compliant solutions. All 19 devices released the inversion/eversion DOF of the ankle, although through different solutions.

III. Misalignment and Interaction Assessment

A. Materials and Methods

1) Participants and Protocol: Misalignment and interactions were assessed on 10 young male healthy subjects (180.3 $\pm$ 4.0 cm, 81.1 $\pm$ 10.1 kg, and 25.8 $\pm$ 4.4 years old). All

participants were healthy without reporting any known locomotion or balance impairment, and they had not suffered any musculoskeletal injury in the previous six months. Participants were chosen with similar shank lengths (35.1 $\pm$ 3.18 cm) and perimeters (38.5 $\pm$ 2.59 cm) to ensure that the devices were fixed in approximately similar anatomical regions. All participants were informed of the study's objectives and methodology and were provided with an informed consent form, which they read and signed. The participants were asked to perform three walking trials at self-selected speed, followed by three walking trials at 1.6 km/h (cadence of 70 beats/minute).

2) Introduction on AFOs: The experimental protocol included three AFOs, two in-house models, and the ankle module of the H2 active exoskeleton (figure 2).

(a) SOF device. (b) SOL device. (c) H2 device.

Fig. 2: AFOs included in the experimental protocol.

The two in-house models innovate in the H2 design by introducing a shin guard and a foot modulus based on a sports shoe. The two in-house prototypes were denominated SOF and SOL, according to the locations of their shin-guard location (frontal or lateral, respectively). Shin guard location is the only difference between these two prototypes.

3) Instrumentation and Data Collection: A motion capture system with 12 cameras (Oqus, Qualisys – Motion-Capture System, Göteborg, Sweden) capturing at 100 Hz was used to measure human lower-limb kinematics during the trials, as well as orthosis kinematics (e.g. robotic joint position in space). Overall, 30 markers were used on the human body and 9 markers were used for each of the prototypes. All markers were placed by the same operator using the anatomical standards described in [43].

Pressures at the interfaces between the user and the device were measured by a system of 8 circular FSRs and processed by an Arduino Nano microcontroller board operating at 100 Hz. Each sensor was labeled from 1 to 8 and fixed to the AFOs's fixations (i.e. straps and shin guards). The FSRs were placed in anatomical areas where high-pressure values should be avoided due to the increased risk of discomfort and lesion [6], [44], [45], e.g. bony prominences in the user's shank. The placement was done by the same operator throughout the protocol to reduce the occurrence of occasional and systematic errors, prior to the donning of the device by the user. Once the user donned the device, the sensors were repositioned according to the user's anatomy. Since recorded pressures and pain thresholds vary greatly with the type and stiffness of tissue they are applied to [3], [8], [44], an effort was done to place the sensors in the same anatomical area for each subject. The comfort and satisfaction questionnaire included 13 questions, scored through a 4-point Liker-scale (Strongly Disagree, Disagree, Agree, and Strongly Agree). Literature research was done on available questionnaires for assessing user satisfaction with AFOs. Since no questionnaire that targeted AFOs directly was found, a choice was made to use questions from the two available questionnaires indicated in [46] as "Generic Questionnaires", defined as the ones for use across all types of orthotic devices and clinical conditions. As such, the questionnaire is based on the adapted CSD-OPUS [47], with one question from the QUEST 2.0 questionnaire [48], pertaining to the device's dimensions. Furthermore, the two questions pertaining to comfort and fitness from the CSD-OPUS were expanded into two new questions, one assessing the foot modulus and one assessing the shank modulus, in order to better assess the differences between AFOs.

B. Results

1) Misalignment and Displacement Measures: Misalignment distance, misalignment angle, strap displacement and shin-guard/strap angular displacement were averaged for 10 subjects and plotted for each orthosis. The initial misalignments captured were -1.11 cm, -0.90 cm, and -0.48 cm horizontally and -1.75 cm, -1.82 cm, and -2.76 cm vertically, for SOF, SOL, and H2, respectively. Regarding these measures, there are differences between devices in misalignment distance (Mz). H2 is the AFO that presents the highest misalignment, at the beginning and trough out the gait cycle. Results also show also shows that the misalignment distance is not constant across gait. Misalignment angles showed that the H2 device has the highest misalignment angle. There are no apparent differences between SOF and SOL. For the displacement values, H2 has higher displacement paths (Dx, Dy, and Dz) and angles (Dα, Dβ, and Dγ) overall, with no differences between the two in-house models. These two measures indirectly represent interactions between the fixations and the user's soft tissues.

2) Pressure on Human-AFO Interface: FSRs in similar anatomical regions were grouped into four different groups, each corresponding to a section of the user's shank: anterior proximal, anterior distal, posterior proximal, and posterior distal. By analyzing the peak values it is verified that the SOF device had lower pressure for all of the four groups, while SOL and H2 have somewhat similar results for the posterior groups. The biggest differences are for sensors of the anterior groups, mainly due to the fitness of the frontal shin-guard compared with the other two fixation mechanisms. This is in opposition to both posterior groups, where sensors were placed at the same type of fixations.

3) Questionnaire on User's Satisfaction: Each participant assessed comfort for each orthosis after roughly the same amount of time wearing the three devices. Direct comparisons between the scores of SOF-H2 and SOF-SOL showed clear differences. First, SOF has largely higher scores than H2 in relation to the foot module, shank module, and overall comfort and fitness, with scores more than 1 point apart on the Likert

scale. These questions also had higher scores than the average difference between questions. On the other hand, SOF has largely higher scores than SOL with regards to pain during the device's use, ability to don the device, the fitness of the device (question 10), and presence of abrasions and irritation.

C. Discussion

Misalignment and Displacement Measures: Motion data analysis allows making direct conclusions regarding misalignment and relative displacement between the fixations and the human limb. Misalignment measures show differences in the Z axis, with both SOF and SOL devices having a smaller initial misalignment in comparison with H2, with no apparent differences for the Y axis. Initial misalignments are around 1 and 1.5 cm for My and Mz, respectively, which is within the values found in literature [19], [28]. Furthermore, misalignment during gait is not constant. This agrees with what is stated in the literature [6], [13]. In fact, this variation during gait is likely due to either slippage of the connections and/or migration of the ICR of the biological which, due to the kinematic mismatch between both joints, is not followed by the AFO [49]. For the Z axis, misalignment diminishes in the H2 device during the swing phase of the gait. However, it is important to note that, during this gait phase, theoretical power transmission for the robotic joint to the user or vice-versa is not significant. In fact, it is to be expected that the largest torques are present during stance and, as such, misalignment during this phase will lead to higher spurious forces and torques at the pHRI than during the swing phase. As such, SOF and SOL have a lower misalignment in the stance phase, indicating lower misalignment-related interactions at the pHRI. Overall, there is a need for manual alignment in all three devices. Furthermore, high misalignment variation can be identified across gait.

Displacement along the Z axis is the value that can more closely be correlated with sheer or friction interactions (as described in [8]) and, as such, is the most important to consider. The results show higher displacements along the Z axis for H2 during the initial stance phases and for SOF and SOL around the beginning of the swing phase. Nevertheless, the displacements are very small in magnitude, and differences between maximum displacements between H2, SOF, and SOL are within 2 mm, which cannot be separated from some systematic or occasional error that could have occurred, as shown in [33]. As such, in this analysis, all three devices have approximately the same behavior. The displacements recorded are within the range present in other studies [33], [34]. Regarding displacement rotations, differences were only observed around the sagittal plane. This is to be expected since it is the motion plane where actuation happens in the case of H2, which can result in an increase in relative movement. Nevertheless, all three curves for the three measures have approximately the same behavior and values, and as such, an exact conclusion cannot be made regarding which device has the lowest displacement rotations.

Pressure on Human-AFO Interface: Pressure data analysis shows fewer pressure interactions for the frontal design (SOF), then the lateral design (SOL), and then the H2 design. Safety assessment, however, is also fundamental, to ascertain if the pressures recorded are below recognized safety values [6], [10]. Recorded values are largely below the PTT values from single-point algometry [50]. These results can be a good initial benchmark to assess safety and pain onset but do not directly correlate to exoskeleton fixations [10]. Further data from circumferential algometry for both healthy and subjects with chronic pain problems were considered, through values found in [51], [52]. The SOF device showed results where the average value plus one standard deviation for all four shin-guard locations is below the pain detection threshold for healthy subjects. The same occurs for patients that suffer from chronic pain except for the posterior proximal group. For the SOL AFO, only the posterior proximal group has an average plus standard deviation below pain detection thresholds for healthy individuals, with results from the anterior distal group being close to the upper bound of pain tolerance threshold (PTT) for chronic pain patients. This can largely be attributed to the type and material of fixation, an important factor in pressure distribution [10], [11]. Finally, the value for the anterior proximal group of the H2 device surpasses safety levels even in healthy subjects, which is a major counter indication for its use. Furthermore, the posterior groups show values close to detection thresholds, another contraindication. The main difference between SOF and SOL can be attributed to the different materials of the straps since these devices report similar misalignments. However, pressures recorded for the H2 device are higher than both SOF and SOL, which can be explained in part by the misalignment reported previously. In fact, while the polymer of the straps in the SOL device is in direct contact with the user's skin, the H2 straps have foam pads to increase comfort [53], which does not translate to lower pressures. This can indicate that these pressures are due to spurious forces in relation to misalignment.

Questionnaire on User's Satisfaction: Questionnaire results show higher comfort scores for the SOF device. Furthermore, the comparison with H2 shows valid shank and foot design choices. Both the introduction of a shin guard against the straps and a commercially available running shoe against the H2's shoe sole seems to reduce the user's discomfort. Furthermore, the main differences between SOF and SOL lie in the fixations at the level of the shin guard. While the frontal model relies on Velcro fixations, the lateral model relies on straps made of a stiffer polymer and a tighter fit, resulting ultimately in pain, discomfort, abrasions, and irritations, in accordance with the higher pressure values recorded. Furthermore, by having the shin guard located laterally, the anterior straps are in contact with the bony prominences of the tibia, which have lower thresholds for pain. This is in contrast to the SOF design, where the location of the shin guard ensures a better distribution of pressures, reducing pain and discomfort. These results are especially important because they indicate not general discomfort but concrete pain and lesions. Two studies

[40], [54] have used the NASA TLX questionnaire, which assesses task load, and a simple 0-100 analog scale for comfort. However, when these studies found significant comfort scores between test conditions, no significant difference was found in NASA TLX scores. On the other hand, the questionnaire used in this work found significant differences between the three devices regarding user satisfaction and allowed to assess which device's characteristics most contributed to these devices. This has not been observed in the literature. As such, the SOF device has been shown to score higher regarding the user's comfort perception, while also showing higher scores for the occurrence of pain and pressure-related lesions. Within the scope of research done, this is the first work that proposes a correlation between the results of these questionnaires and misalignment.

IV. Alignment Solutions

The initial design of the SOF device is in figure 3.

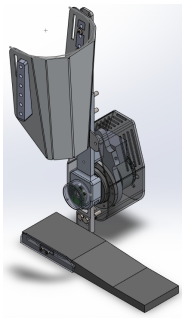

Fig. 3: Initial CAD design of the SOF AFO.

A. Materials and Methods

1) Mechanical Design of Alignment Solutions: By considering the misalignment requirements and the alignment solutions reviewed in the section "Related Work", this work idealized and designed 5 alignment solutions: 3 manual alignment solutions ("Adjust joint's vertical position", "Adjust joint's horizontal position" and "Adjust shin guard position") and 2 solutions based on kinematic redundancy ("Release Iv/Ev trough a revolute joint" and "Introduce a prismatic joint"). All solutions and simulations were designed in SolidWorks 2021®(Dassault Systèmes, Vélizy-Villacoublay, France). Data from the experimental protocol was used to guide the dimensioning of solutions. To do this, three measures were calculated: initial vertical misalignment, initial horizontal misalignment, and maximum vertical displacement. These measures correlate with solutions "Adjust joint's vertical position", "Adjust joint's horizontal position", and "Introduce a prismatic joint", respectively. Alignment solution 1 ("Adjust joint's vertical position") was developed considering the measure "Vertical initial misalignment". This measure indicates an initial misalignment that ranges from -2.89 cm to -0.62 cm. As such, there is a need to increase the Z coordinate of the robotic joint. The main purpose of this solution is to allow for this vertical adjustment. This solution was realized by adding six sets of screw holes at the connection between the footplate and the motor connector plate. These screw holes are 0.5 cm apart and allow for vertical regulation of the motor connector plate. The height of the motor connector plate was kept the same, while the cut that supports the screws was increased by 1 cm. As such, the height of the motor connector plate can now vary from the initial position to 2.5 cm above the initial position. The initial design did not allow for height adjustment of the robotic joint.

Alignment solution 2 ("Adjust joint's horizontal position") was developed considering the measure "Horizontal initial misalignment". This measure indicates an initial misalignment that ranges from -1.9 cm to -0.31 cm. As such, the horizontal position of the joint should be adaptable, which is the purpose of this solution. In the initial design, the footplate is connected to the shoe through an outsole plate with. The current design does not allow for horizontal adjustment of this outsole plate. Furthermore, while the used CAD model of the outsole plate only includes two M3 screw holes, the prototype used in the experimental protocol realizes this connection through five screws. This was replicated in the final design by replacing the two initial holes with the five of the final prototype. While the centers of the initial holes were 1.22 cm apart, those of the final design were 0.5 cm apart. Finally, four more screw holes were within the same distance, and the length of the outsole plate was increased by 2 cm. This realized the alignment solution by allowing the user to adjust the horizontal position of the robotic joint to a maximum of 2 cm in steps of 0.5 cm.

The alignment solution "Adjust shin guard Position" allows for better alignment of the shin guard. Since the fixation realized by the shin guard is rather rigid, its contact with low-compliant tissues will lead to increased interactions, and, as such, a fitting of the shin guard in softer tissue is necessary to increase comfort. From the protocol, it was found that the subject with the lowest shank length had the shin guard in contact with his knee joint. This subject had a height of 1.70, which is within the range of heights allowed by the initial design [22]. The initial design allowed only lowering the height of the shin guard by 0.9 cm by providing an additional screw hole at the connection between the shin guard and the proximal upright. It was found to not be sufficient to prevent contact with less compliant tissue close to the knee joint. As such, the height of the shin guard should be adaptable, which is the main purpose of this solution. This was done by adding an additional hole at the connection between the shin guard and the proximal upright of the AFO and two additional screw holes at the connection between the proximal upright and the distal motor connector plate. Each of these alterations allowed the shin guard to be lowered an additional 0.9 cm. The final design allows lowering the shin guard by a total of 3.6 cm, whereas the initial design only allowed for 0.9 cm.

The solution "Release inversion/eversion through a revolute joint" was developed to partly solve the kinematic mismatch between the user and the AFO. This solution released the inversion/eversion DOF by introducing a revolute joint at the footplate level, designed by splitting the footplate structure in

two. The axis of this joint was kept perpendicular to the plane of actuation to avoid the transmission of actuation torque to this DOF. A more complex design with mechanical end stops should still be implemented in order to increase the safety and applicability of the solution.
Finally, the solution "Introduce a prismatic joint" was designed considering the measure "Maximum vertical displacement". This measure indicates a cuff displacement between -0.97 and 0.33 cm. As such, this displacement should be eliminated since it correlates with shear forces at the pHRI. The low vertical compliance of the initial design does not allow for compensation for this displacement. A prismatic DOF was introduced in the shank structure of the AFO, of which the main purpose is to compensate for the measured displacement. This solution consists of a rail mechanism between the shin guard and the proximal upright. The proximal upright of the shank structure was cut following the guide's geometry and functions as the rail, while an additional part was introduced between this bard and the shin guard fixation that functions as the guide. This guide is fixed to the structure through screws, following the same mechanisms as the initial design. The prismatic joint has a vertical ROM of 1 cm, following the requirements set.

2) Validation of Alignment Solutions: To validate the solutions "Adjust joint's vertical position", "Adjust joint's horizontal position" and "Adjust shin guard position", it is necessary to guarantee the mechanical integrity of the structure. As such, mechanical simulations were made using the simulation tool from SolidWorks 2021®(Dassault Systèmes, Vélizy-Villacoublay, France). These simulations were based on previous work done in this prototype by [22] by applying a torque of 65 N.m. where the actuation module would be. The appropriate fixations and connections were applied according to the simulations described in [22].
The solutions "Release inversion/eversion through a revolute joint" and "Introduce a prismatic joint" were validated through motion tests. To do this, a model of the human foot and leg was imported into the CAD software and fixed to the sole. For the revolute joint solution, the angle between the leg and the foot was increased and decreased by 25° (above biological levels [55]) and an interference test was done between the foot and leg models and the orthosis structure. This test assesses the ROM of the implemented revolute joint by recording the angles where there is a collision between the leg or foot and the AFO. The study was done at 60 frames per second for 15 seconds. Within the first five seconds, the joint performed an eversion motion, followed by an inversion motion during the next five seconds towards the initial position and an eversion motion for the last five seconds. For the prismatic joint solution, the leg model was fixed to the posterior face of the shin guard and the guide position was set at 0.5 cm below the top of the rail. The model was set to rotate 12 ° in each direction in the frontal plane, thus provoking a linear movement of the guide. An interference check between the guide and the top and bottom parts of the rail was done. This allowed assessing the compensation ability of the rail. Finally, the final prototype with all five solutions implemented was validated through a mechanical simulation study. The same torque, fixations, and connections as in the previous mechanical tests were applied for this final validation.

B. Results

In order to guarantee that the structures subject to mechanical tests kept their integrity under the applied stresses, a factor of safety (FoS) of 1.5 was selected as the threshold to validate each solution. This FoS is defined as the quotient between the material's yield strength and the calculated Von Mises stress. The lowest FoS for the validation of the vertical alignment solution was 1.682, above the set threshold. Furthermore, the FoSs for the footplate and the outsole plate at the connection were, respectively, 1.81 and 1.27. The FoS at the connection for the footplate is above the set threshold, while the one for the outsole plate is not. Similarly, simulation results for the shin guard alignment solution found the lowest FoS to be equal to 1.705, which is higher than the defined threshold.
The results of the motion study for the revolute joint solution found initial interference at around 8° for eversion and 9° for inversion. While biological ROMs for these DOFs are higher than these values [56], a study has found that during human gait the ROMs of eversion and inversion are around 5° [57]. Thus, the ROM of this solution was deemed sufficient for the application. The motion study results for the prismatic joint solution found initial interference at around 8° for the positive rotation and 9° for the negative rotation. These results were found to be appropriate, since the prismatic joint managed to compensate for the full one cm set as a requirement, converting a rotation movement of the model into a linear movement of the guide. For the simulation that validates the final design, the lowest FoS was 0.7 at the level of the revolute joint, which is below the threshold defined.

C. Discussion

The design for the alignment solution "Adjust joint's vertical position" has been proven to allow an initial vertical alignment within the requirements defined. Furthermore, mechanical stress tests have shown that structural integrity is kept under the expected stresses of normal use. This solution is, as such, fully developed for manufacturing and implementation into the current design. Within literature. manual alignment solutions allow only for vertical alignment so that the device is usable by subjects of different heights. The literature's manual alignment solutions are not implemented directly to align the robotic and user's joints. As such, the range of these solutions is not stated. Furthermore, within the scope of research done, this work is the first to utilize experimental data to dimension a vertical manual alignment solution. The two studies referenced for direct assessment of misalignment through motion capture used this technique to validate previously designed alignment solutions [19], [28].
The alignment solution "Adjust joint's horizontal position" fully realizes the requirements defined. Although the FoS of the outsole plate was below the defined threshold, a choice

was made that the design had sufficient mechanical stability. In fact, while the original prototype had not been validated in [22], real-life tests were done after production. Part of these tests was done through the experimental protocol in the previous section, where it was proven that prolonged use of the AFO did not compromise its structural integrity. Furthermore, the same prototype was tested with an initial version of the actuation module, wherein the actuator applied a torque similar to the real use case. Test results showed that the structural integrity of the fixation between the footplate and the outsole plate was not compromised. Since the new design does not change the structure significantly, a choice was made to accept the current design as safe. This solution is fully realized and ready to be produced and implemented. From the literature, no horizontal alignment solution was found. Since no study used direct misalignment assessment to dimension manual alignment solutions, a hypothesis for the lack of horizontal alignment solutions is that, visually, horizontal misalignment is not evident. As such, it is possible that the authors of these studies did not find a need for this kind of solution. Nevertheless, this work shows that such a solution is needed and should be implemented.

The alignment solution "Adjust shin guard position" fully realizes the objective of the user being allowed to lower the vertical position of the shin guard. Furthermore, the stress studies proved that the implemented solution did not compromise the structural integrity of the design. As such, this solution is fully realized and ready for production. The original design from [22] only allowed the shin guard's position to be increased by only 4.5 cm. This work proves that an adaptation that lowers the shin guard's position is necessary to better realize the structure's design to a wider range of users.

The kinematic redundancy solution that releases inversion/eversion rotations was implemented according to the high variability of misalignment during gait and due to its frequent use in the literature. Motion studies showed a ROM of 8° for eversion and 9° for inversion, before the user's limb reaches the shin guard, which is adequate for anatomic gait. However, the ROM of the implemented joint is 360°, since no mechanical end stops were implemented. The full anatomical ROM of the inversion/eversion DOF of the ankle joint is between 25° and 30° for eversion and around 52° for inversion [55]. As such, solutions from the literature have implemented mechanical end-stops for these joints to avoid safety hazards [58] [59]. Study [13] states that designed solutions should not have a larger workspace than the user's joint. As such, these safety features should be implemented into the current design before production.

The solution "Introduce a prismatic joint" fully realizes the requirements defined. Furthermore, this solution increases the overall mass of the AFO by approximately 74 grams, representing an 8% increase from the original mass of 917 grams (excluding the actuation modulus). No similar solution was found in the literature for AFOs. This is mainly due to the need to first assess the displacement to properly dimension the solution, which was not done. Nevertheless, study [19] describes the validation of a similar solution for a knee exoskeleton. The study reported that its alignment solution weighed 190 grams. Although the solution included, besides a prismatic joint, two revolute joints, these were directly implemented on existing braces. As such, it is expected that the prismatic joint is the main contributor to this added mass. The solution in [19] represents a mass that doubles that of the solution here described. Nevertheless, its validation showed improved comfort and performance [54]. As such, the weight of the implemented solution may not be problematic for real-life validation. Nevertheless, a mechanism that prevents the guide from escaping the rail through its top opening should still be implemented before production.

Finally, the validation results for the final design show a FoS above the required threshold for all components except the revolute joint. However, as described before, this solution is not fully realized, since the current design still needs the implementation of mechanical end stops. As such, a follow-up study of the mechanical stability of the final design with a new iteration of the revolute joint solution is still required. In fact, this next iteration should also increase the mechanical durability of this connection.

V. Conclusions and Future Work

A. Conclusions

This work had three distinct parts, each corresponding to a different section presented before. The work in each section was done towards the main goal, to develop solutions that would solve the misalignment problem in an AFO prototype. In the section "Related Work", first, a comprehensive review of misalignment causes and effects on the basis of literature was given. It was found that human-robot joint misalignment is inevitable and that it arises from the impossibility of, initially, properly aligning the two joints and from the inherent kinematic mismatch of the two structures. Furthermore, the literature shows that this phenomenon leads to spurious forces and torques at the level of the interface between the human and the exoskeleton. These interactions are one of the main reasons behind user abandonment of these devices since they greatly compromise the user's comfort during use and can even pose a safety risk to the user. Secondly, a comprehensive review of misalignment and interaction assessment strategies was done. Five different measures were found to assess misalignment: direct misalignment assessment through motion capture; fixation displacement through motion capture; pressure assessment through FSR sensors; shear stresses assessment through load cells; musculoskeletal interaction assessment through a dummy limb. Finally, the state-of-the-art on alignment solutions in AFO and exoskeletons was presented. It was found that all devices implemented manual alignment solutions. Furthermore, a majority introduced an additional inversion/eversion DOF to partly solve the kinematic mismatch between the human-robot systems. This implementation was done either through the introduction of compliant materials at the joint level or through revolute joints. Finally, soft exoskeletons are still in an early phase of research but are

increasingly looking for a viable alternative to anthropomorphic exoskeletons to solve misalignment issues.

In the section "Misalignment and Interaction Assessment", human-AFO misalignment and interactions were assessed in an experimental environment for the three different prototypes. The protocol followed the recommendations on misalignment assessment from the literature, by using motion capture data to assess misalignment and displacement, FSRs to collect pressure and interactions in pHRI, and a comfort and satisfaction questionnaire to assess user's perception of the prototypes. It was found that the SOF design performed better in most measures, namely misalignment, pressure interactions, and fixation displacements. Furthermore, it was the AFO with the higher satisfaction level rated by the participants. As such, this device was chosen to develop the alignment solutions. Experimental results also contributed to identifying the magnitude values and, as such, guided the design of alignment solutions.

Finally, in the section "Alignment Solutions", five different alignment solutions were designed using the orientations from the previous sections and, when applicable, properly validated. These comprised three manual alignment solutions that allowed the user to adjust both joint and shin-guards position, a solution based on a revolute joint that released the inversion/eversion DOF of the joint, and a prismatic joint that compensated from the maximum vertical displacement captured in the protocol. All solutions, when applicable, passed their validation tests. The three manual alignment solutions are ready for production and implementation, while the remaining solutions need further work to make them more robust for real-life use.

B. Future Work

First, an analysis of all three devices after the in-house models have their actuation modules implemented should be done, since it is not clear if the results would be significantly different. Furthermore, a direct assessment of shear stresses should be done, since it will allow a better assessment of the interactions. Finally, the gait kinematics captured from the protocol and the treadmill data have yet to be analyzed. Since each device is expected to have a significant effect on normal gait kinematics, this analysis should be done. Nevertheless, remarkably different conclusions are not expected to be reached, since misalignment is closely related to human-robot kinematics. Regarding the implementation of alignment solutions, the three manual alignment solutions are ready for production and implementation, while the remaining two need further work to increase their safety and usability. Finally, validation of each solution in a real-life setting should be done.

REFERENCES

[1] N. Smidt, H. C. de Vet, L. M. Bouter, and J. Dekker, "Effectiveness of exercise therapy: A best-evidence summary of systematic reviews," *Australian Journal of Physiotherapy*, vol. 51, no. 2, pp. 71–85, 2005. [Online]. Available: https://www.sciencedirect.com/science/article/pii/S0004951405700362

[2] A. Ashburn, C. Partridge, and L. D. Souza, "Review article : Physiotherapy in the rehabilitation of stroke: a review," *Clinical Rehabilitation*, vol. 7, no. 4, pp. 337–345, 1993. [Online]. Available: https://doi.org/10.1177/026921559300700410

[3] A. Trulsson Schouenborg, M. Rivano Fischer, E. Bondesson, and A. Jöud, "Physiotherapist-led rehabilitation for patients with chronic musculoskeletal pain: interventions and promising long-term outcomes," *BMC Musculoskelet Disord*, vol. 22, no. 1, p. 910, Oct. 2021.

[4] M. Volpini, V. Bartenbach, M. Pinotti, and R. Riener, "Clinical evaluation of a low-cost robot for use in physiotherapy and gait training," *J Rehabil Assist Technol Eng*, vol. 4, p. 2055668316688410, Jan. 2017.

[5] G. Morone, S. Paolucci, A. Cherubini, D. De Angelis, V. Venturiero, P. Coiro, and M. Iosa, "Robot-assisted gait training for stroke patients: current state of the art and perspectives of robotics," *Neuropsychiatr Dis Treat*, vol. 13, pp. 1303–1311, May 2017.

[6] E. Rocon, A. F. Ruiz, R. Raya, A. Schiele, J. L. Pons, J. M. Belda-Lois, R. Poveda, M. J. Vivas, and J. C. Moreno, *Human–Robot Physical Interaction*. John Wiley & Sons, Ltd, 2008, ch. 5, pp. 127–163. [Online]. Available: https://onlinelibrary.wiley.com/doi/abs/10.1002/9780470987667.ch5

[7] N. Postol, S. Lamond, M. Galloway, K. Palazzi, A. Bivard, N. J. Spratt, and J. Marquez, "The metabolic cost of exercising with a robotic exoskeleton: A comparison of healthy and neurologically impaired people," *IEEE Trans Neural Syst Rehabil Eng*, vol. 28, no. 12, pp. 3031–3039, Jan. 2021.

[8] N. Jarrassé and G. Morel, "Connecting a human limb to an exoskeleton," *IEEE Transactions on Robotics*, vol. 28, pp. 697–709, 2012, adding passive DOFs.

[9] B. Phillips and H. Zhao, "Predictors of assistive technology abandonment," *Assistive technology : the official journal of RESNA*, vol. 5, pp. 36–45, 02 1993.

[10] J. Bessler, G. B. Prange-Lasonder, L. Schaake, J. F. Saenz, C. Bidard, I. Fassi, M. Valori, A. B. Lassen, and J. H. Buurke, "Safety assessment of rehabilitation robots: A review identifying safety skills and current knowledge gaps," *Frontiers in Robotics and AI*, vol. 8, 3 2021.

[11] J. Bessler, G. B. Prange-Lasonder, R. V. Schulte, L. Schaake, E. C. Prinsen, and J. H. Buurke, "Occurrence and type of adverse events during the use of stationary gait robots—a systematic literature review," *Frontiers in Robotics and AI*, vol. 7, 11 2020.

[12] J. Wang, X. Li, T. H. Huang, S. Yu, Y. Li, T. Chen, A. Carriero, M. Oh-Park, and H. Su, "Comfort-centered design of a lightweight and backdrivable knee exoskeleton," *IEEE Robotics and Automation Letters*, vol. 3, pp. 4265–4272, 10 2018.

[13] M. B. Naf, K. Junius, M. Rossini, C. Rodriguez-Guerrero, B. Vanderborght, and D. Lefeber, "Misalignment compensation for full human-exoskeleton kinematic compatibility: State of the art and evaluation," *Applied Mechanics Reviews*, vol. 70, 9 2018, needs more reading.

[14] M. Cempini, S. M. M. D. Rossi, T. Lenzi, N. Vitiello, and M. C. Carrozza, "Self-alignment mechanisms for assistive wearable robots: A kinetostatic compatibility method," *IEEE Transactions on Robotics*, vol. 29, pp. 236–250, 2013.

[15] D. H. Wang, J. Guo, K. M. Lee, C. J. Yang, and H. Yu, "An adaptive knee joint exoskeleton based on biological geometries," *Proceedings - IEEE International Conference on Robotics and Automation*, pp. 1386–1391, 2011.

[16] A. Schiele and F. C. V. D. Helm, "Kinematic design to improve ergonomics in human machine interaction," *IEEE Transactions on Neural Systems and Rehabilitation Engineering*, vol. 14, pp. 456–469, 12 2006.

[17] D. Zanotto, Y. Akiyama, P. Stegall, and S. K. Agrawal, "Knee joint misalignment in exoskeletons for the lower extremities: Effects on user's gait," *IEEE Transactions on Robotics*, vol. 31, pp. 978–987, 8 2015, done, see one note.

[18] A. Schiele and F. C. van der Helm, "Influence of attachment pressure and kinematic configuration on phri with wearable robots," *Applied Bionics and Biomechanics*, vol. 6, pp. 157–173, 2009.

[19] S. V. Sarkisian, M. K. Ishmael, G. R. Hunt, and T. Lenzi, "Design, development, and validation of a self-aligning mechanism for high-torque powered knee exoskeletons," *IEEE Transactions on Medical Robotics and Bionics*, vol. 2, pp. 248–259, 5 2020.

[20] "Technaid - h2 exoskeleton," https://www.technaid.com/products/robotic-exoskeleton-exo-exoesqueleto/.

[21] "Birdlab - smartos project," http://birdlab.dei.uminho.pt/smartos//.

[22] C. E. Ribeiro, "Design of a wearable active ankle-foot orthosis for both sides," Master's thesis, Universidade do Minho, Guimarães, Portugal, Apr. 2021.

[23] J. S. C. Figueiredo, "Smart wearable orthosis to assist impaired human walking," Ph.D. dissertation, Universidade do Minho, Guimarães, Portugal, Jul. 2019.

[24] N. Itoh, D. Imoto, S. Kubo, K. Takahashi, N. Hishikawa, Y. Mikami, and T. Kubo, "Gait training using a stationary, one-leg gait exercise assist robot for chronic stroke hemiplegia: a case report," *J Phys Ther Sci*, vol. 30, no. 8, pp. 1046–1051, Jul. 2018.

[25] R. Berriozabalgoitia, B. Sanz, A. B. Fraile-Bermúdez, E. Otxoa, I. Yeregui, I. Bidaurrazaga-Letona, I. Duñabeitia, A. Antigüedad, M. Domercq, J. Irazusta, and A. Rodriguez-Larrad, "An overground robotic gait training program for people with multiple sclerosis: A protocol for a randomized clinical trial," *Front Med (Lausanne)*, vol. 7, p. 238, Jun. 2020.

[26] Y. He, D. Eguren, T. P. Luu, and J. L. Contreras-Vidal, "Risk management and regulations for lower limb medical exoskeletons: a review," *Med Devices (Auckl)*, vol. 10, pp. 89–107, May 2017.

[27] M. Cenciarini and A. M. Dollar, "Biomechanical considerations in the design of lower limb exoskeletons," *IEEE International Conference on Rehabilitation Robotics*, 2011.

[28] J. Bessler-Etten, L. Schaake, G. B. Prange-Lasonder, and J. H. Buurke, "Assessing effects of exoskeleton misalignment on knee joint load during swing using an instrumented leg simulator," *Journal of NeuroEngineering and Rehabilitation*, vol. 19, p. 13, 12 2022, done, see one note. [Online]. Available: https://jneuroengrehab.biomedcentral.com/articles/10.1186/s12984-022-00990-z

[29] A. Rathore, M. Wilcox, D. Z. M. Ramirez, R. Loureiro, and T. Carlson, "Quantifying the human-robot interaction forces between a lower limb exoskeleton and healthy users," *Proceedings of the Annual International Conference of the IEEE Engineering in Medicine and Biology Society, EMBS*, vol. 2016-October, pp. 586–589, 10 2016.

[30] M. Wilcox, A. Rathore, D. Z. M. Ramirez, R. C. Loureiro, and T. Carlson, "Muscular activity and physical interaction forces during lower limb exoskeleton use," *Healthcare Technology Letters*, vol. 3, pp. 273–279, 2016.

[31] Y. Wang, J. Qiu, H. Cheng, and X. Zheng, "Analysis of human–exoskeleton system interaction for ergonomic design," *Human Factors*, 2020.

[32] L. Armitage, S. Turner, and M. Sreenivasa, "Human-device interface pressure measurement in prosthetic, orthotic and exoskeleton applications: A systematic review," *Medical Engineering and Physics*, vol. 97, pp. 56–69, 11 2021.

[33] M. Cempini, A. Marzegan, M. Rabuffetti, M. Cortese, N. Vitiello, and M. Ferrarin, "Analysis of relative displacement between the hx wearable robotic exoskeleton and the user's hand jner journal of neuroengineering and rehabilitation analysis of relative displacement between the hx wearable robotic exoskeleton and the user's hand," *Journal of NeuroEngineering and Rehabilitation*, vol. 11, p. 147, 2014. [Online]. Available: http://www.jneuroengrehab.com/content/11/1/147http://www.jneuroengrehab.com/content/11/1/147

[34] Y. Akiyama, Y. Yamada, and S. Okamoto, "Interaction forces beneath cuffs of physical assistant robots and their motion-based estimation," *Advanced Robotics*, vol. 29, pp. 1315–1329, 10 2015.

[35] M. Ferrarin, J. Stallard, R. Palmieri, and A. Pedotti, "Estimation of deformation in a walking orthosis for paraplegic patients," *Clinical Biomechanics*, vol. 8, no. 5, pp. 255–261, 1993. [Online]. Available: https://www.sciencedirect.com/science/article/pii/026800339390035G

[36] G. Katsube, S. Qi, T. Itami, K. Yano, I. Mori, and K. Kameda, "Ankle foot orthosis that prevents slippage for tibial rotation in knee osteoarthritis patients," in *2021 43rd Annual International Conference of the IEEE Engineering in Medicine & Biology Society (EMBC)*, 2021, pp. 4728–4731.

[37] B. Celebi, M. Yalcin, and V. Patoglu, "Assiston-knee: A self-aligning knee exoskeleton," in *2013 IEEE/RSJ International Conference on Intelligent Robots and Systems*, 2013, pp. 996–1002.

[38] J. Schorsch, A. Keemink, A. Stienen, F. van der Helm, and D. Abbink, "A novel self-aligning mechanism to decouple force and torques for a planar exoskeleton joint," *Mechanical Sciences*, vol. 5, pp. 29–35, 08 2014.

[39] Schiele, *An Explicit Model to Predict and Interpret Constraint Force Creation in pHRI with Exoskeletons*. IEEE Xplore, 2008.

[40] A. Schiele, "Ergonomics of exoskeletons: Subjective performance metrics," *2009 IEEE/RSJ International Conference on Intelligent Robots and Systems, IROS 2009*, pp. 480–485, 12 2009.

[41] A. Mahmoudi Khomami and F. Najafi, "A survey on soft lower limb cable-driven wearable robots without rigid links and joints," *Robotics and Autonomous Systems*, vol. 144, p. 103846, 2021. [Online]. Available: https://www.sciencedirect.com/science/article/pii/S0921889021001317

[42] M. D. C. Sanchez-Villamañan, J. Gonzalez-Vargas, D. Torricelli, J. C. Moreno, and J. L. Pons, "Compliant lower limb exoskeletons: a comprehensive review on mechanical design principles," *J Neuroeng Rehabil*, vol. 16, no. 1, p. 55, May 2019.

[43] H. Tsushima, M. E. Morris, and J. Mcginley, "Test-retest reliability and inter-tester reliability of kinematic data from a three-dimensional gait analysis system," *J Jpn Phys Ther Assoc*, vol. 6, pp. 9–17, 2003.

[44] D. L. Bader, P. R. Worsley, and A. Gefen, "Bioengineering considerations in the prevention of medical device-related pressure ulcers," *Clinical Biomechanics*, vol. 67, pp. 70–77, 7 2019.

[45] P. C. Silva, M. T. Silva, and J. M. Martins, "Evaluation of the contact forces developed in the lower limb/orthosis interface for comfort design," *Multibody System Dynamics*, vol. 24, pp. 367–388, 10 2010.

[46] E. Bettoni, G. Ferriero, H. Bakhsh, E. Bravini, G. Massazza, and F. Franchignoni, "A systematic review of questionnaires to assess patient satisfaction with limb orthoses," *Prosthetics and Orthotics International*, vol. 40, pp. 158–169, 4 2016.

[47] "Orthotics prosthetics users survey," https://www.sralab.org/rehabilitation-measures/orthotics-prosthetics-users-survey.

[48] "Quebec user evaluation of satisfaction with assistive technology." [Online]. Available: https://www.sralab.org/rehabilitation-measures/quebec-user-evaluation-satisfaction-assistive-technology

[49] T. Lee, I. Kim, and Y. S. Baek, "Design of a 2dof ankle exoskeleton with a polycentric structure and a bi-directional tendon-driven actuator controlled using a pid neural network," *Actuators*, vol. 10, pp. 1–17, 1 2021.

[50] R. P. J. M. Belda-Lois and M. J. Vivas, *Case Study: Analysis of Pressure Distribution and Tolerance Areas for Wearable Robots*. John Wiley & Sons, Ltd, 2008, ch. 5, pp. 127–163. [Online]. Available: https://onlinelibrary.wiley.com/doi/abs/10.1002/9780470987667.ch5

[51] T. Kermavnar, V. Power, A. de Eyto, and L. O'Sullivan, "Computerized cuff pressure algometry as guidance for circumferential tissue compression for wearable soft robotic applications: A systematic review," *Soft Robotics*, vol. 5, 10 2017.

[52] T. Kermavnar, V. Power, A. D. Eyto, and L. W. O'Sullivan, "Computerized cuff pressure algometry as guidance for circumferential tissue compression for wearable soft robotic applications: A systematic review," *Soft Robotics*, vol. 5, pp. 1–16, 2 2018.

[53] M. Bortole, A. Venkatakrishnan, F. Zhu, J. C. Moreno, G. E. Francisco, J. L. Pons, and J. L. Contreras-Vidal, "The h2 robotic exoskeleton for gait rehabilitation after stroke: Early findings from a clinical study wearable robotics in clinical testing," *Journal of NeuroEngineering and Rehabilitation*, vol. 12, 6 2015.

[54] S. V. Sarkisian, M. K. Ishmael, and T. Lenzi, "Self-aligning mechanism improves comfort and performance with a powered knee exoskeleton," *IEEE Transactions on Neural Systems and Rehabilitation Engineering*, vol. 29, pp. 629–640, 2021.

[55] J. Jiang, K. M. Lee, and J. Ji, "Review of anatomy-based ankle–foot robotics for mind, motor and motion recovery following stroke: design considerations and needs," *International Journal of Intelligent Robotics and Applications*, vol. 2, pp. 267–282, 9 2018.

[56] J. Dul and G. Johnson, "A kinematic model of the human ankle," *Journal of Biomedical Engineering*, vol. 7, no. 2, pp. 137–143, 1985. [Online]. Available: https://www.sciencedirect.com/science/article/pii/0141542585900433

[57] L. Moreira, J. Figueiredo, P. Fonseca, J. P. Vilas-Boas, and C. Santos, "Lower limb kinematic, kinetic, and emg data from young healthy humans during walking at controlled speeds," *Scientific Data*, vol. 8, p. 103, 04 2021.

[58] S. Christensen, S. Rafique, and S. Bai, "Design of a powered full-body exoskeleton for physical assistance of elderly people," *International Journal of Advanced Robotic Systems*, vol. 18, 2021.

[59] A. C. Satici, A. Erdogan, and V. Patoglu, "Design of a reconfigurable ankle rehabilitation robot and its use for the estimation of the ankle impedance," *2009 IEEE International Conference on Rehabilitation Robotics, ICORR 2009*, pp. 257–264, 2009.